ISTANBUL TECHNICAL UNIVERSITY ★ GRADUATE SCHOOL OF SCIENCE
ENGINEERING AND TECHNOLOGY

INCREASING MAGNETIC DIPOLE MOMENT OF YOUNG NEUTRON STARS: IMPLICATIONS FOR PULSAR BRAKING INDICES

M.Sc. THESIS

Abdullah GÜNEYDAŞ

Physics Engineering Department

Physics Engineering Programme

JUNE 2012

ISTANBUL TECHNICAL UNIVERSITY ★ GRADUATE SCHOOL OF SCIENCE
ENGINEERING AND TECHNOLOGY

INCREASING MAGNETIC DIPOLE MOMENT OF YOUNG NEUTRON STARS: IMPLICATIONS FOR PULSAR BRAKING INDICES

M.Sc. THESIS

Abdullah GÜNEYDAŞ
(509091121)

Physics Engineering Department

Physics Engineering Programme

Thesis Advisor: Assoc. Prof. Dr. Kazım Yavuz EKŞİ

JUNE 2012

İSTANBUL TEKNİK ÜNİVERSİTESİ ★ FEN BİLİMLERİ ENSTİTÜSÜ

ARTAN MANYETİK DİPOL MOMENTLERİNİN ATARCA FRENLEME İNDİSLERİ ÜZERİNDEKİ ETKİSİ

YÜKSEK LİSANS TEZİ

Abdullah GÜNEYDAŞ
(509091121)

Fizik Mühendisliği Anabilim Dalı

Fizik Mühendisliği Programı

Tez Danışmanı: Doç. Dr. Kazım Yavuz EKŞİ

HAZİRAN 2012

Abdullah GÜNEYDAŞ, a M.Sc. student of ITU Graduate School of Science, Engineering and Technology 509091121, successfully defended the thesis entitled **"INCREASING MAGNETIC DIPOLE MOMENT OF YOUNG NEUTRON STARS: IMPLICATIONS FOR PULSAR BRAKING INDICES"**, which he prepared after fulfilling the requirements specified in the associated legislations, before the jury whose signatures are below.

Thesis Advisor :	**Assoc. Prof. Dr. Kazım Yavuz EKŞİ** İstanbul Technical University	....
Jury Members :	**Prof. Dr. Ali ALPAR** Sabancı University	....
	Prof. Dr. Ahmet Togo GİZ İstanbul Technical University	....

Date of Submission : **04 May 2012**
Date of Defense : **08 June 2012**

FOREWORD

I wish to thank Assoc. Prof. Dr. Kazım Yavuz EKŞİ who was not only a supervisor, he also encouraged and guided me throughout this thesis and my academic life. This thesis could not have been written without his struggle.

June 2012 Abdullah GÜNEYDAŞ

TABLE OF CONTENTS

Page

ABBREVIATIONS

PSR	: Pulsating Source of Radio (Pulsar)
RPP	: Rotation Powered Pulsar
CCO	: Central Compact Object
AXP	: Anomalous X-ray Pulsar
SGR	: Soft Gamma-ray Repeater
SN	: Supernova
SNR	: Supernova Remnant
MDR	: Magnetic Dipole Radiation
ATNF	: Australia Telescope National Facility

LIST OF TABLES

LIST OF FIGURES

Page

INCREASING MAGNETIC DIPOLE MOMENT OF YOUNG NEUTRON STARS: IMPLICATIONS FOR PULSAR BRAKING INDICES

SUMMARY

A nascent neutron star may suffer fallback accretion soon after the proto-neutron star stage. This hypercritical accretion episode can submerge the magnetic field deep in the crust. The diffusion of the magnetic field back to the surface will take hundreds to millions of years depending on the amount of accretion and consequently the depth the field is submerged. The field growth timescale (τ) of the field will be short if the star had a brief accretion episode and vice verse. We investigate the physical motivation behind two models for the growth of the magnetic dipole moment μ: $\mu = \mu_{\rm max} - (\mu_{\rm max} - \mu_{\rm min})\exp(-t/\tau)$ and $\mu = \mu_{\rm min} + (\mu_{\rm max} - \mu_{\rm min})\exp(-\tau/t)$. We study the implications of these models on pulsar spin parameters (especially on braking index). The former model is ruled out investigating measured spin parameters of PSR B1509$-$58. The latter model is investigated further with its implications on pulsar evolution on $P-\dot{P}$ diagram. If the star has a large kick velocity less amount of fallback accretion will occur. We thus expect that there should be an inverse relation between the transverse velocity and the field growth timescale. Assuming the braking indices less than 3 are due to the growth of the dipole moment we infer the growth time-scale for each pulsar with measured braking indices. We seek for a relation between the measured transverse velocities and the inferred field growth timescales. As Crab has a precisely known age and a measured second deceleration parameter it is possible to determine its magnetic field growth timescale as well as the ratio of maximum and minimum field values. We find that the latter is < 1.5 indicating that the magnetic field of Crab and possibly all rotationally powered pulsars change by only a small factor. For B0833$-$45 (Vela), B0540$-$69, J0537$-$6910 and J1846$-$0258 which lack m measurement but have measured braking indices and estimations for their true ages, we determined the minimum value of allowed $\mu_{\rm max}/\mu_{\rm min}$ ratios, which are 4.90, 1.40, 10.5 and 1.83, respectively. $(\mu_{\rm max}/\mu_{\rm min})_{\rm min} = 10.5$ for J0537$-$6910, can provide motivation for future works questioning transition between different neutron star families.

May 2012 Abdullah Güneydaş

ARTAN MANYETİK DİPOL MOMENTLERİNİN ATARCA FRENLEME İNDİSLERİ ÜZERİNDEKİ ETKİSİ

ÖZET

Atarcaların, hızla spin atan, yüksek manyetik alana sahip nötron yıldızları olduğu, 1967 sonunda Antony Hewish ve Joselyn Bell tarafından ilk gözlemlenişlerinden kısa süre sonra anlaşıldı. Onları gözlemlememizi sağlayan radyo ışımalarını yapmak için harcadıkları enerji sebebiyle, atarcaların spin frekansları sürekli düşer. Atarca manyetik alanını, yıldızın merkezinde ideal bir manyetik dipol varsayıp modellersek (manyetik dipol ışıması modeli), spin evrimi için

$$\frac{d}{dt}\left(\frac{1}{2}I\Omega^2\right) = -\frac{2\mu_\perp^2}{3c^3}\Omega^4$$

denklemine ulaşırız; burada Ω açısal spin frekansı, $\mu_\perp$ açısal hız vektörüne dik manyetik dipol momenti bileşeni, I atarcanın eylemsizlik momenti ve c ışık hızıdır.

Frenleme indisi, $n \equiv \Omega\ddot{\Omega}/\dot{\Omega}^2$, atarca spin evrimi incelenirken yaygın olarak kullanılan bir gözlemsel parametredir. Manyetik dipol ışıması modeli frenleme indisi için $n = 3$ sonucu verir. Fakat hiçbir atarca için $n = 3$ değeri gözlemlenememiştir: bütün gözlemler $n < 3$ vermektedir; hatta PSR J1734$-$3333 için $n = 0.9 \pm 0.2$, J0537$-$6910 için $n = -1.5$ ve Vela Atarcası için $n = 1.4 \pm 0.2$ gibi 3'e görece uzak gözlemler mevcuttur. Bu gözlemler manyetik dipol ışıması modelinin atarca frenleme indislerini tek başına açıklamadaki yetersizliğine işaret eder.

Frenleme indisinin 3'den küçük oluşunu açıklamak için birçok model önerilmiştir. Bu modeller 2 grupta toplanabilirler: İlk grup modeller manyetik dipol ışıması ile birlikte yıldızın spinini düşürecek başka bir etkiyi daha hesaba katar; bu diğer etki yıldızın etrafındaki bir kütle aktarım diski ya da yıldızın saçtığı relativistik parçacıklar olabilir. İkinci grup modeller ise manyetik dipol ışıması modelini geliştirir; bu, merkezde ideal dipol yerine sonlu manyetize küre almakla veya dipol momentinin zaman içinde değiştiğini varsayarak olabilir. Buradaki çalışmamızda biz, manyetik dipol momentinin zaman içinde artması durumunu inceleyeceğiz.

Yeni doğmuş bir nötron yıldızı, kendisini oluşturan süpernova patlamasında kurtulma hızına ulaşamamış maddeyi üzerine aktarabilir. Böyle bir madde aktarma dönemi nötron yıldızının manyetik alanını kabuğunun derinliklerine gömebilir. Alanın yeniden yüzeye çıkışı, aktarılan madde miktarı ve alanın ne kadar derine gömüldüğüne bağlı olarak, yüzlerce hatta milyonlarca yıl alabilir. Eğer kütle aktarım aşaması kısa sürdüyse manyetik dipol momenti büyüme zaman ölçeği τ kısa olacaktır. Atarcaların doğumlarına neden olan süpernova patlaması sırasında aldıkları hız ne kadar büyük olursa, kütle aktarımları o kadar küçük, bundan dolayı gömülü manyetik alanlarının yüzeye çıkması için gerekli zaman da o kadar kısa olacaktır. Çalışmamızda bu ilişkiyi

sorguladık ve veri azlığına rağmen böyle bir ilişkiden bahsedilebileceğini iddia ettik. Daha çok veri ile yanlışlanmaması halinde bu ilişki frenleme indislerinin 3'den küçük oluşunu açıklamaya çalışan birçok model arasında manyetik alan artışı öngörenleri öne çıkaracaktır.

Bu çalışmada, derine gömülmüş bir manyetik alanın tekrar yüzeye çıkışı için iki ayrı modeli ($\mu = \mu_{\rm max} - (\mu_{\rm max} - \mu_{\rm min})\exp(-t/\tau)$ ve $\mu = \mu_{\rm min} + (\mu_{\rm max} - \mu_{\rm min})\exp(-\tau/t)$), arkalarındaki fiziksel motivasyonu ve atarca spin mekanizmaları üzerindeki öngörülerini de araştırarak inceledik. Modellerden ilki PSR B1509−58'in spin parametreleri kullanılarak yanlışlandı. İkinci model üzerine olan incelememize, atarcaların $P-\dot{P}$ diagramı üzerindeki evrimine yaptığı etkiyi kattık. Hem yaşı hem de ikinci frenleme indisi ($m \equiv \Omega^2\dddot{\Omega}/\dot{\Omega}^3$) bilinen tek atarca olduğu için sadece Yengeç Atarcası'nın model parametreleri tam olarak hesaplanabildi; maksimum manyetik dipol momentinin minimum manyetik dipol momentine oranının 1.5'den küçük ($\mu_{\rm max}/\mu_{\rm min} = 1.31$) olduğu görüldü. Model parametrelerini belirlemek için gerekli olan ölçüm sayısından bir eksik ölçüme sahip atarcalar için, $\mu_{\rm max}/\mu_{\rm min}$ oranını farklı değerlerde sabitleyip bilinmeyen sayısını 1 azaltmak suretiyle τ'yu hesaplayıp, $P-\dot{P}$ diagramı üzerinde her τ değerine karşılık gelen atarca evrimini çizdik. Bu atarcalardan sadece ikinci frenleme indisi ölçümü eksik olanları için maksimum manyetik dipol momentinin minimum manyetik dipol momentine oranı, $(\mu_{\rm max}/\mu_{\rm min})_{\rm min}$, B0833−45 (Vela) için 4.90, B0540−69 için 1.40, J0537−6910 için 10.5 ve J1846−0258 için 1.83 olarak belirlendi; bu sayede $\mu_{\rm max}/\mu_{\rm min}$'in sabitleneceği değerler için bir alt limit elde etmiş olduk. $\mu_{\rm max}/\mu_{\rm min}$'in sabitleneceği değerler,sadece ikinci frenleme indisi ölçümü eksik olan atarcalar için $(\mu_{\rm max}/\mu_{\rm min})_{\rm min}$ değeri ve bu değerden büyük olan 1.5, 3, 5, 10, 30, 100, 1000 değerleri olarak şeçildi. Yaşı için bir tahmin bulunmayan PSR B1509−58 için ise böyle bir alt limit belirlenemediği için doğrudan 1.5, 3, 5, 10, 30, 100, 1000 değerleri kullanıldı.

$P-\dot{P}$ diagramları üzerindeki evrim çizgileri, $\mu = \mu_{\rm min} + (\mu_{\rm max} - \mu_{\rm min})\exp(-\tau/t)$ şeklindeki manyetik dipol momenti artış modelimizin frenleme indislerinin 3'den küçük oluşunu açıklamanın yanında, AXP (anormal x-ışını atarcaları) ve SGR (tekrarlayan yumuşak gama ışın kaynakları) gibi bazı nötron yıldızı sınıflarının oluşumunu da aydınlatabileceğini gösterdi; diagramlardan $\mu_{\rm max}/\mu_{\rm min}$ oranı yüksek olduğunda radyo atarcalarının diagramın AXP veya SGR yoğunluklu bölgesine doğru evrileceği görülüyor. Son olarak J0537−6910 için $(\mu_{\rm max}/\mu_{\rm min})_{\rm min} = 10.5$ gibi yüksek bir $\mu_{\rm max}/\mu_{\rm min}$ alt limiti bulunması bu ihtimali güçlendirir nitelikte.

Mayıs 2012 Abdullah Güneydaş

1. INTRODUCTION

Neutron stars are born in supernova explosions as first suggested by Baade and Zwicky in 1934 [2]. This was spectacularly confirmed by the discovery of the Crab Pulsar [3] at the center the Crab Nebula which is known to be born in 1054 AD according to Chinese records. Soon after the discovery of radio pulsars by Anthony Hewish and his graduate student Jocelyn Bell [4] their nature as rapidly rotating highly magnetized neutron stars radiating at the expense of their rotational energy was established [5]. According to magnetic dipole radiation (MDR) model these rotationally powered pulsars (RPPs) spin-down acoording to

$$\frac{d}{dt}\left(\frac{1}{2}I\Omega^2\right) = -\frac{2\mu_\perp^2}{3c^3}\Omega^4 \tag{1.1}$$

where Ω is the angular spin frequency, $\mu_\perp$ is the dipole magnetic moment perpendicular to the spin angular velocity vector, I is the moment of inertia of the star and c is the speed of light.

An observational dimensionless parameter related to the spin-down torques on these RPPs is the braking index which is operationally defined as

$$n \equiv \frac{\Omega\ddot{\Omega}}{\dot{\Omega}^2}. \tag{1.2}$$

The value of n should be 3 if RPPs are spinning down with MDR. Most of the measured pulsar braking indices are close to 3 but slightly less [6–8] as shown in Table 1.1. This indicates that some other process is contributing to the MDR in braking these objects. The recently measured braking index of PSR J1734$-$3333 as $n = 0.9 \pm 0.2$ [9] and that of J0537$-$6910 as $n = -1.5$ [10] together with the earlier measurement as $n = 1.4 \pm 0.2$ of the Vela Pulsar [11] indicate that this process might severely alter the spin history of young neutron stars.

Table 1.1: Pulsars with accurately measured braking indices.

Pulsar	ν (Hz)	$\dot{\nu}$ ($\times 10^{-11} s^{-2}$)	n	m	Age (years)	$v_{\perp}$ (km s^{-1})	References
B0531+21(Crab)	30.2254	-38.6228(3)	2.51(1)	10.2(1)	939	140±8	[6, 12]
B1509−58	6.61151524	-6.6943713	2.832(3)	17.6(19)	*	*	[13]
B0833−45(Vela)	11.2(5)	-1.57(2)	1.4(2)	*	$2 \pm 1 \times 10^4$	62±2	[11, 14, 15]
B0540−69	19.738	-18.6560(5)	2.087(7)	*	950±150	1300±612	[14, 16]
J0537−6910	62.0375	-19.760	-1.5	*	∼5000	634±50	[10, 14, 17]
J1846−0258	3.07434(1)	-6.69678(5)	2.65(1)	*	≥2000	*	[7, 18]
J1119−6127	2.451203	-2.415507(1)	2.684(2)	*	*	*	[8]
J1734−3333	0.85518	-16.6702(3)	0.9(2)	*	*	*	[9]

Numbers in parenthesis are last digit errors.

Another observational clue to the nature of the spin-down of a RPP is the second deceleration parameter [19],

$$m \equiv \frac{\Omega^2 \dddot{\Omega}}{\dot{\Omega}^3}, \tag{1.3}$$

which the MDR model predicts to be $m = 15$. The second deceleration parameter has been measured from only two RPPs: $m = 17.6 \pm 1.9$ for PSR B1509−58 [13] and $m = 10.2 \pm 0.1$ for the Crab pulsar [6].

The arguments for addressing what makes the braking indices of RPPs somewhat less than 3 can broadly be classified into two categories. The first type of arguments invoke an additional torque assisting the MDR torque either due to ejection of relativistic particles [20] or the presence of a putative debris disk [21–24]. The second type of arguments invoke a modification to the simple MDR model either by time dependent magnetic fields [19, 25, 26] or the finite size effect of dipole due to the presence of the corotating plasma [27]. Note that this is a very broad scheme and e.g. the model by Wu et al. (2003) that employs torque contributions from pulsar emission models has ingredients from both classes [28].

If the magnetic dipole moment of a pulsar is changing in time, the braking index becomes

$$n = 3 - 2\frac{\dot{\mu}}{\mu}\frac{P}{\dot{P}} \tag{1.4}$$

where $P = 2\pi/\Omega$ is the rotation period of the neutron star. Defining

$$\tau_c \equiv \frac{P}{2\dot{P}} \tag{1.5}$$

and

$$\tau_\mu \equiv \frac{\mu}{\dot{\mu}} \tag{1.6}$$

Equation (**1.4**) becomes

$$\tau_\mu = \tau_c \frac{4}{3-n}. \tag{1.7}$$

The second deceleration parameter in the case of changing magnetic moments is

$$m = 9n - 12 + \frac{(3-n)^2}{2}\left(1 + \frac{\mu\ddot{\mu}}{\dot{\mu}^2}\right) \tag{1.8}$$

In Table 1.1 we show the RPPs with measured braking indices.

A common ingredient of supernova models is the fallback of some material that can not reach the escape velocity [29]. The initial accretion rate of fallback matter can be very large and can submerge any magnetic field that was formed in the proto-neutron star stage [30]. The diffusion of this field back to the surface will be on an Ohmic timescale which depends on the conductivity which in turn depends on density. This will lead to a delayed amplification of the field. The delayed amplification of the magnetic dipole field was already suggested [31,32] to explain the lack of detection of a pulsar in SN87a.

In this thesis, the mechanism in which braking indices less than 3 are due to increasing dipole moments [19, 25, 26] is investigated. The dipole moment of RPPs could be growing because it was submerged [30] in the crust due to fallback accretion [29] following the supernova explosion. According to Chevalier, the fallback due to the reversed shock in SN87A reached to the surface of the neutron star 2 hours after bounce and the initial accretion rate was $320 M_{\odot}\mathrm{yr}^{-1}$ [33]. The amount of matter that will reach the surface and the time required for this to happen will vary depending on many details like the kick velocity, magnetic field just before fallback and spin frequency of the neutron star [34]. In cases of heavy accretion, similar to that of SN 87A, the preexisting magnetic field that was formed in the proto-neutron star stage will be submerged to the crust and the diffusion of the field back to the surface will take 100s to millions of years, depending on the conductivity of the crust and the depth of submergence which in turn depends on the amount of fallback [30, 35]. If the initial accretion rate estimated by Chevalier is typical then even magnetar like fields, $B \sim 10^{15}$ G, that were formed in the proto-neutron star stage can be submerged [33]. This leads us to the conclusion that the kick velocity is the most important factor determining the amount of fallback mass that will accrete onto the neutron star. Neutron stars with large kick velocities will acquire smaller amount of mass during the fallback accretion stage and time-scale for the growth of their field will be shorter. This leads to the prediction that there should be an anti-correlation between the transverse velocities and the time-scale for the growth of the dipole moment.

If one assumes that the braking indices are to be understood by the growth of the magnetic dipole moment [19,25,26,36], one can infer the timescale for the growth of the magnetic dipole moments. In Chapter 4 we seek a relation between this inferred timescale τ for the field growth and the measured transverse velocities indicating that RPPs with larger transverse velocities have smaller field growth time scales as predicted above. In Chapter 2 we employ a field growth model to calculate the evolution of RPPs on the $P - \dot{P}$ diagram for a range of field growth time-scales in Chapter 3.

More recently, it is understood that a substantial fraction of young neutron stars do not manifest themselves as RPPs the prototypical of which is the Crab pulsar. The so called magnetars (see [37] for a review) obviously are young neutron stars with characteristic ages $\tau_c \sim 10^4$ years as inferred from their large spin-down rates. Magnetars are characterized by their super-Eddington bursts attributed to their high magnetic fields. Yet another probably related family of young neutron stars are the central compact objects (CCOs) in supernova remnants (see [38] for a review) whose magnetic fields are inferred to be very low (see e.g. [39]) and are dubbed anti-magnetars. The growth of the magnetic field of CCOs are studied recently [36]. There is strong evidence for the existence of a strong sub-surface magnetic field as inferred from the anomalously large ($\sim 64\%$) pulsed fraction of the surface emission of the CCO in Kes 79 [40], much larger than the magnetic field inferred from the spin-down [39]. CCOs might then be the progenitors of some RPPs or even magnetars assuming the subsurface field diffuses to the surface in a Hubble time.

2. EVOLUTION OF THE MAGNETIC FIELD

In this chapter we discuss the evolution of the magnetic field in the crust. Our analysis is based on [36, 41]. The evolution of the magnetic field is governed by the induction equation

$$\frac{\partial \mathbf{B}}{\partial t} = -\nabla \times (\eta \nabla \times \mathbf{B}), \tag{2.1}$$

where

$$\eta = \frac{c^2}{4\pi\sigma} \tag{2.2}$$

is the magnetic diffusivity, σ being the conductivity. As the crust is solid we neglect the fluid motion. We assume the magnetic field inside the star is dipolar. This also is the assumption in all similar calculations (e.g. [36]). The dipolar field can be derived from the azimuthal vector potential

$$\mathbf{A} = B_* R^2 s(r,t) \frac{\sin\theta}{r} \hat{\phi} \tag{2.3}$$

as

$$\mathbf{B} = B_* R^2 \left(\frac{2s}{r^2} \cos\theta \, \hat{\mathbf{r}} - \frac{1}{r} \frac{\partial s}{\partial r} \sin\theta \, \hat{\theta} \right) \tag{2.4}$$

where B_* is the magnetic field before the fallback accretion. Assuming $\sigma = \sigma(r)$ a diffusion equation is established for s:

$$\frac{\partial s}{\partial t} = \eta \left(\frac{\partial^2 s}{\partial r^2} - \frac{2s}{r^2} \right). \tag{2.5}$$

The boundary conditions are

$$\frac{\partial s}{\partial r} + \frac{s}{r} = 0 \qquad \text{at} \qquad r = R \tag{2.6}$$

and $s \to$ constant in the deep interior.

Two kinds of approach to the solution of the diffusion Equation (**2.5**) will lead to two different ways the field evolves at the surface. If one seeks a solution with separation of variables via $s(r,t) = \mathscr{T}(t)\mathscr{R}(r)$ then the time component will have an equation of the form $d\mathscr{T}/dt = \mathscr{T}/\tau$ which will lead to exponential solutions for s and consequently B. This implies a model of field growth as

$$\mu(t) = \mu_{\rm max} - (\mu_{\rm max} - \mu_{\rm min})\exp\left(-\frac{t}{\tau}\right), \qquad \text{Model I} \tag{2.7}$$

a model employed in many work (e.g. [42]). This field growth model can be ruled out by using the measured properties of B1509−58 given in Table 1.1: Equation (**1.7**) implies that $\mu/\dot{\mu} = 37265$ years for B1509−58. Using this in Equation (**1.8**) and noting that $\tau = -\dot{\mu}/\ddot{\mu}$ in this field growth model one is led to $\tau < 0$ which is unacceptable.

The numerical results (e.g. [36]) motivate a self-similar evolution of the field. We thus seek a self-similar solution of Equation (**2.5**) assuming magnetic diffusivity, η, is constant. This assumption obviously is not correct as magnetic diffusivity depends on conductivity which in turn depends on density. As we are only interested in the evolution of the field at the surface of the NS, the whole effect of these will be swept into τ which is a free parameter of the model that we try to determine observationally. In order to apply a similarity analysis we have to put Equation (**2.5**) into dimensionless form. We define

$$\Sigma = \frac{s}{s^*}, \qquad \theta = \frac{t}{t^*}, \qquad x = \frac{r}{r^*} \tag{2.8}$$

and choose

$$t^* = \frac{r^{*2}}{\eta}. \tag{2.9}$$

With these definitions the Equation (**2.5**) becomes

$$\frac{\partial \Sigma}{\partial \theta} = \frac{\partial^2 \Sigma}{\partial x^2} - \frac{2\Sigma}{x^2}. \tag{2.10}$$

We define a self-similarity variable

$$\xi = x\theta^{-\lambda} \tag{2.11}$$

and change variables by using

$$\frac{\partial \Sigma}{\partial \theta} = \frac{d\Sigma}{d\xi}\frac{\partial \xi}{\partial \theta} = -\lambda x \theta^{-\lambda-1}\frac{d\Sigma}{d\xi} \tag{2.12}$$

$$\frac{\partial \Sigma}{\partial x} = \frac{d\Sigma}{d\xi}\frac{d\xi}{dx} = \theta^{-\lambda}\frac{d\Sigma}{d\xi} \tag{2.13}$$

$$\frac{\partial^2 \Sigma}{\partial x^2} = \frac{d^2\Sigma}{d\xi^2}\left(\frac{\partial \xi}{\partial x}\right)^2 + \frac{d\Sigma}{d\xi}\frac{\partial^2 \xi}{\partial x^2} = \frac{d^2\Sigma}{d\xi^2}\theta^{-2\lambda} \tag{2.14}$$

We thus obtain

$$-\lambda \xi \theta^{2\lambda-1}\frac{d\Sigma}{d\xi}=\frac{d^2\Sigma}{d\xi^2}-\frac{2\Sigma}{\xi^2}. \tag{2.15}$$

We see that if we choose

$$\lambda = 1/2 \tag{2.16}$$

the appearance of θ and x disappears in favor of self-similar variable ξ. This yields

$$\frac{d^2\Sigma}{d\xi^2}+\frac{1}{2}\xi\frac{d\Sigma}{d\xi}-\frac{2\Sigma}{\xi^2}=0. \tag{2.17}$$

Equation (**2.17**) has an exact solution

$$\Sigma(\xi)=\xi^{-1}\exp\left(-\frac{\xi^2}{4}\right). \tag{2.18}$$

As a self-similar solution this can not be expected to satisfy the boundary conditions and provide the evolution of the field at the surface. A full solution of the Equation (**2.17**) is also possible in terms of error function. The exponential part $\exp\left(-\xi^2/4\right)$ is always a part of the solution. As $\xi^2 \propto \theta^{-1} \propto t^{-1}$ this motivates a field growth model of the form

$$\mu = \mu_{\min}+(\mu_{\max}-\mu_{\min})\exp\left(-\frac{\tau}{t}\right) \qquad \text{Model II} \tag{2.19}$$

where t is in the denominator of the exponential. Here τ is the time-scale for the diffusion of the field to the surface of the star. This is the field growth model we will use in the following. The two field growth models given in Equations (**2.7**) and (**2.19**) are shown in Figure 2.1 for comparison.

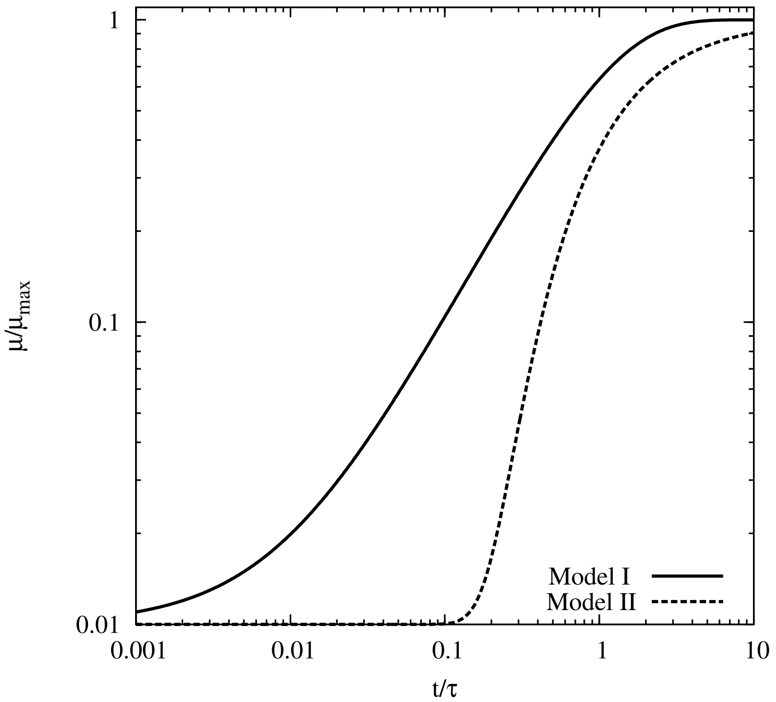

Figure 2.1: The two field growth models given in Equations (**2.7**) and (**2.19**).

3. EVOLUTION OF PULSARS ON THE $P-\dot{P}$ DIAGRAM

In this chapter we investigate the implications of the field growth model given in Equation (**2.19**) for the braking indices and evolution of pulsars on the $P-\dot{P}$ diagram. We provide constraints on the diffusion timescale of the field to the surface hoping this will allow for the estimation of the fallback accretion history of these objects. We note that the relevance of growing magnetic fields for explaining the braking indices is already qualitatively sketched in [9] and further investigated in [26]. Note, however, that the field growth model employed in [26] is different than the field growth model employed in this thesis as given in Equation (**2.19**).

We assume that following the initial heavy fallback the dipole moment of the neutron star has reduced to a low value. We follow the spin evolution while the magnetic field grows from $\mu_{\rm min}$ to its saturation value $\mu_{\rm max}$. The field will then slowly decay but as we are only interested in the episode where the braking indices are less than 3 we are not going to follow the evolution at this stage, nor the field evolution model we employ, given in Equation (**2.19**), can address this stage.

According to the field growth model given in Equation (**2.19**)

$$\frac{\dot{\mu}}{\mu}=\frac{\tau}{t^2}\frac{\mu-\mu_{\rm min}}{\mu}, \tag{3.1}$$

and

$$\frac{\mu\ddot{\mu}}{\dot{\mu}^2}=\frac{\tau-2t}{\tau}\frac{\mu}{\mu-\mu_{\rm min}}. \tag{3.2}$$

Using Equation (**3.1**) in Equation (**1.4**) we obtain

$$n=3-2\frac{P}{\dot{P}}\frac{\tau}{t^2}\frac{\mu-\mu_{\rm min}}{\mu}. \tag{3.3}$$

Similarly, using Equation (**3.2**) in Equation (**1.8**) we obtain

$$m=9n-12+\frac{(3-n)^2}{2}\left(1+\frac{\tau-2t}{\tau}\frac{\mu}{\mu-\mu_{\rm min}}\right). \tag{3.4}$$

Note that, according to Equation (**1.1**), the magnetic moment is given by

$$\mu=\sqrt{\frac{3}{8\pi^2}Ic^3P\dot{P}} \tag{3.5}$$

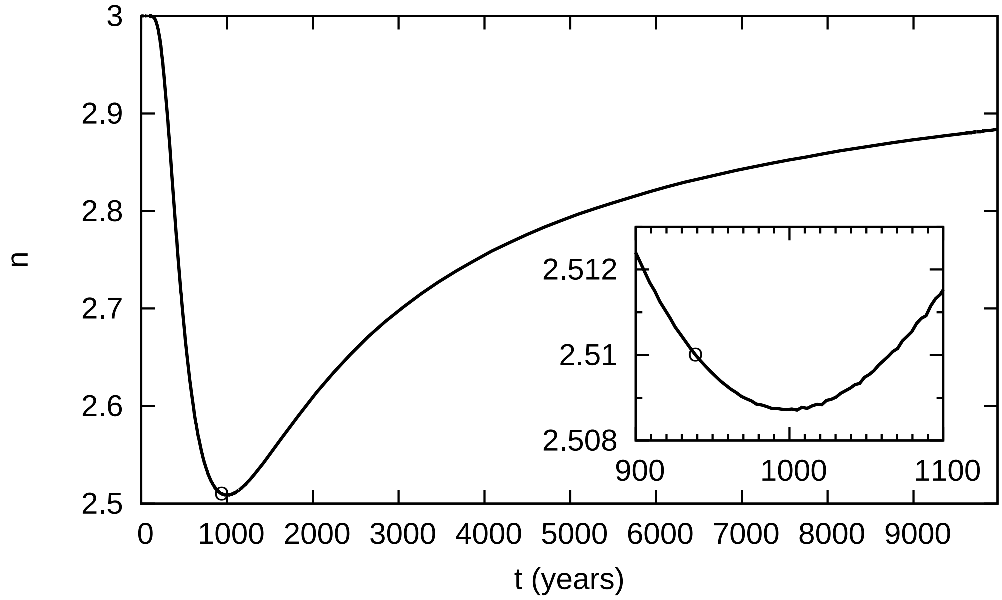

Figure 3.1: Evolution of braking index of Crab Pulsar. Circle marks t_0; 1993 AD, 939 years after the supernova. Small frame on bottom right zooms the main plot about braking index minimum.

Assuming a pulsar was born at $t = 0$ and its age was t_0 at the time corresponding measurements in Table 1.1 were taken, values t_0, ν, $\dot{\nu}$, n and m allow one to calculate $\mu(t_0)$, $\dot{\mu}(t_0)$ and $\ddot{\mu}(t_0)$, which determine model parameters in Equation (**2.19**) (τ, $\mu_{\rm max}$, $\mu_{\rm min}$) for the pulsar.

3.1 Crab Pulsar

The only pulsar for which all the values in Table 1.1 are known is Crab Pulsar (B0531+21). Model parameters calculated by the method just mentioned are $\tau =$ 1508 years, $\mu_{\rm max} = 4.65 \times 10^{30}$ G cm^3 and $\mu_{\rm max}/\mu_{\rm min} = 1.31$ (Figures 3.1, 3.2). Current magnetic moment of Crab Pulsar is $\mu(t_0) = 3.78 \times 10^{30}$ G cm^3, so model predicts approximately 1.23 times further magnetic moment growth. This small ratio $\mu_{\rm max}/\mu_{\rm min}$ for the Crab pulsar implies that this object has suffered a small amount of accretion and its field had been submerged only shallow.

3.2 Pulsars With One Parameter Not Measured

For pulsars other than Crab in Table 1.1, either m or true age is not measured. Searching solutions with fixed $\mu_{\rm max}/\mu_{\rm min}$ ratio decreases the number of parameters in Equation (**2.19**) by one and allows one to find solutions for the pulsars lacking one required datum. Therefore, B1509−58 which lacks age estimation, and B0833−45 (Vela), B0540−69, J0537−6910 and J1846−0258 which lack second deceleration parameter (equivalently $\ddot{\nu}$ or $\dddot{\Omega}$) measurements can be evaluated for different $\mu_{\max}/\mu_{\min}$ ratios.

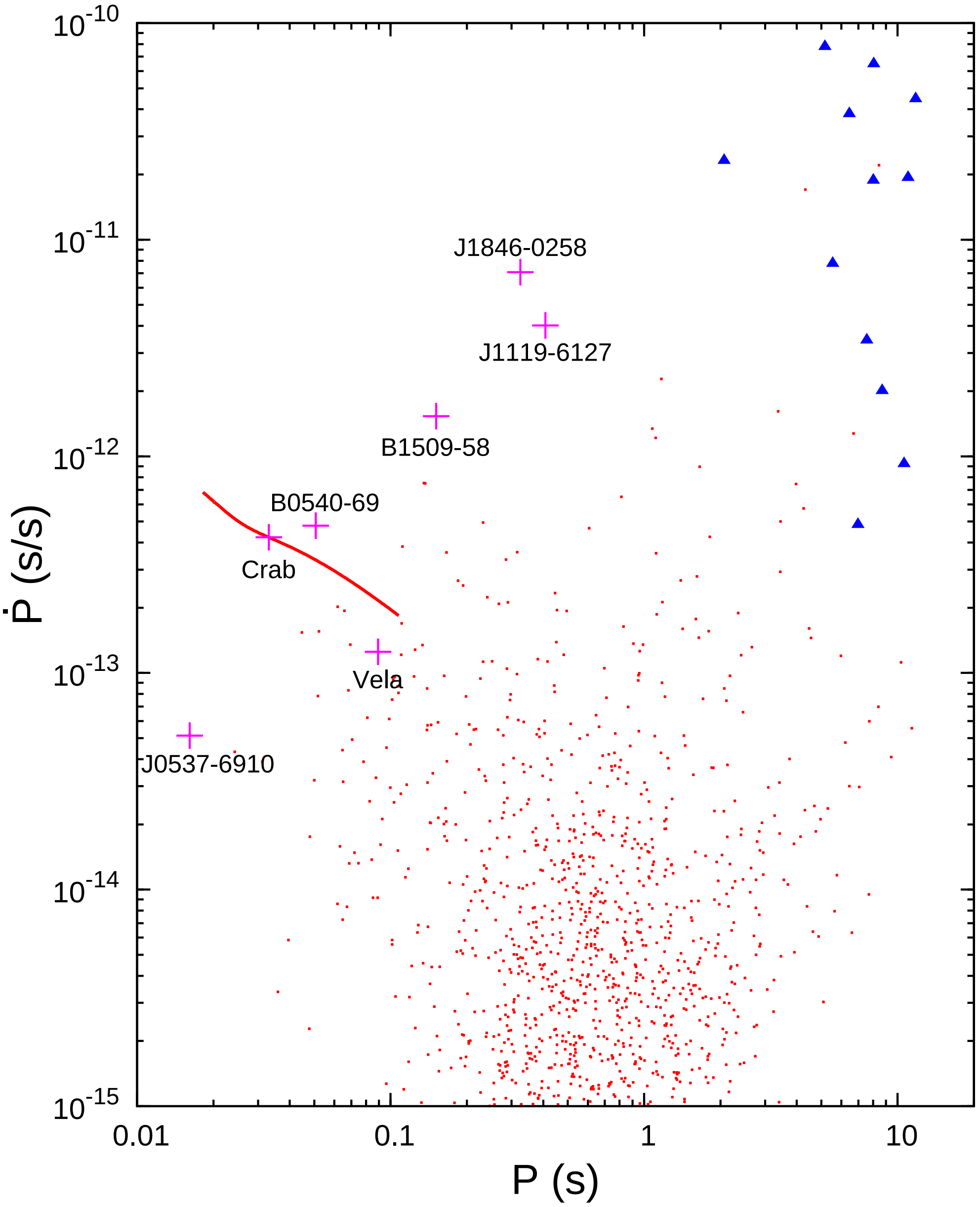

Figure 3.2: Evolution of Crab Pulsar on $P-\dot{P}$ diagram from $t = 1$ year (1055 AD) to $t = 10^4$years. The time when measurements in Table 1.1 were taken corresponds to $t_0 = 939$ years (1993 AD). Dots represent radio pulsars and triangles represent AXPs and SGRs; data taken from ATNF Pulsar Database [1].

For the pulsars which lack only m measurement, $\mu(t_0)$ can be obtained through Equation (**1.1**) and $\dot{\mu}(t_0)$ can be obtained through time derivative of Equation (**1.1**). This allows one to construct relation $\mu_{\rm min}(\tau) = \mu - \dot{\mu}t^2/\tau$ for $t = t_0$ from Equation (**3.1**). $\mu_{\rm min}(\tau)$ allows one to construct $\mu_{\rm max}(\tau)$, via main model Equation (**2.19**). At this point, plot $\mu_{\rm max}/\mu_{\rm min}$ versus τ can be obtained (Figure 3.3). While a positive correlation between $\mu_{\rm max}/\mu_{\rm min}$ and τ is expected, we interpret minimum $\mu_{\rm max}/\mu_{\rm min}$ ratio corresponds to minimum possible τ which is called $\tau_{\rm min}$. We plot evolution of these pulsars and B1509−58 which lacks age estimation, on $P-\dot{P}$ diagram, for the fixed $\mu_{\rm max}/\mu_{\rm min}$ ratios 3, 5, 10, 30, 100, 1000, starting from $\mu_{\rm max}(\tau_{\rm min})/\mu_{\rm min}(\tau_{\rm min})$, which is the smallest value for the $\mu_{\rm max}/\mu_{\rm min}$ ratio (Figures A.1, A.2, A.3, A.4, A.5).

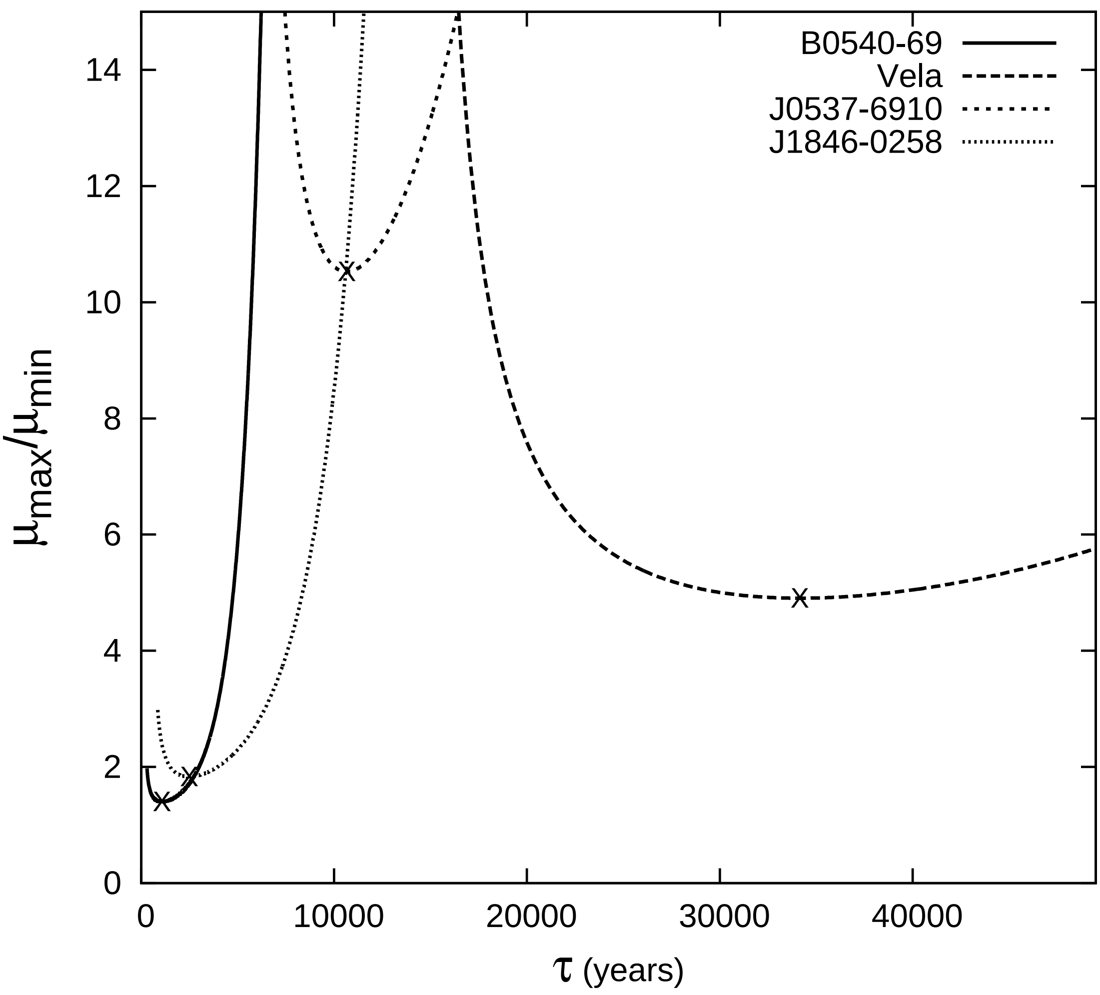

Figure 3.3: $\mu_{\rm max}/\mu_{\rm min}$ versus τ for the pulsars lack only m measurement. "X" marks $\tau_{\rm min}$ for each pulsar.

4. A RELATION BETWEEN KICK VELOCITY AND FIELD GROWTH TIMESCALE

During their formation pulsars get large kicks leading to large space velocities ~ 300 km s^{-1}. A nascent neutron star will accrete less of the fallback material if it is moving rapidly. In the case of Bondi-Hoyle accretion, the accretion rate will be $\dot{M} \propto v^{-3}$. Magnetic dipole moments of neutron stars with large kick velocities will be submerged shallow and will diffuse to the surface in a relatively shorter time than those which have small kick velocities and suffer large amounts of fallback and deep submergence of their field. This predicts an inverse relation between the transverse velocities of RPPs and the growth time-scale of their magnetic moment.

Of the 8 RPPs with measured braking indices we could find only 4 with measured transverse velocities as shown in Table 1.1. Figure 4.1 shows the relation between $\tau_{\rm min}$ and the transverse velocities of these 4 objects. $\tau_{\rm min}$ is only a lower bound of the field growth time-scale τ which can be calculated only for Crab Pulsar. Due to low number of data it is hard to establish a relation, but noting $\tau_{\rm min}$ values of these 4 pulsars except Crab are only lower bounds for τ values, there is no sign of correlation with available data. Moreover, we have to emphasize that the braking index of the Vela pulsar is model dependent [11] and factors like the initial spin and magnetic field are also important in determining the amount of mass accreted via fallback.

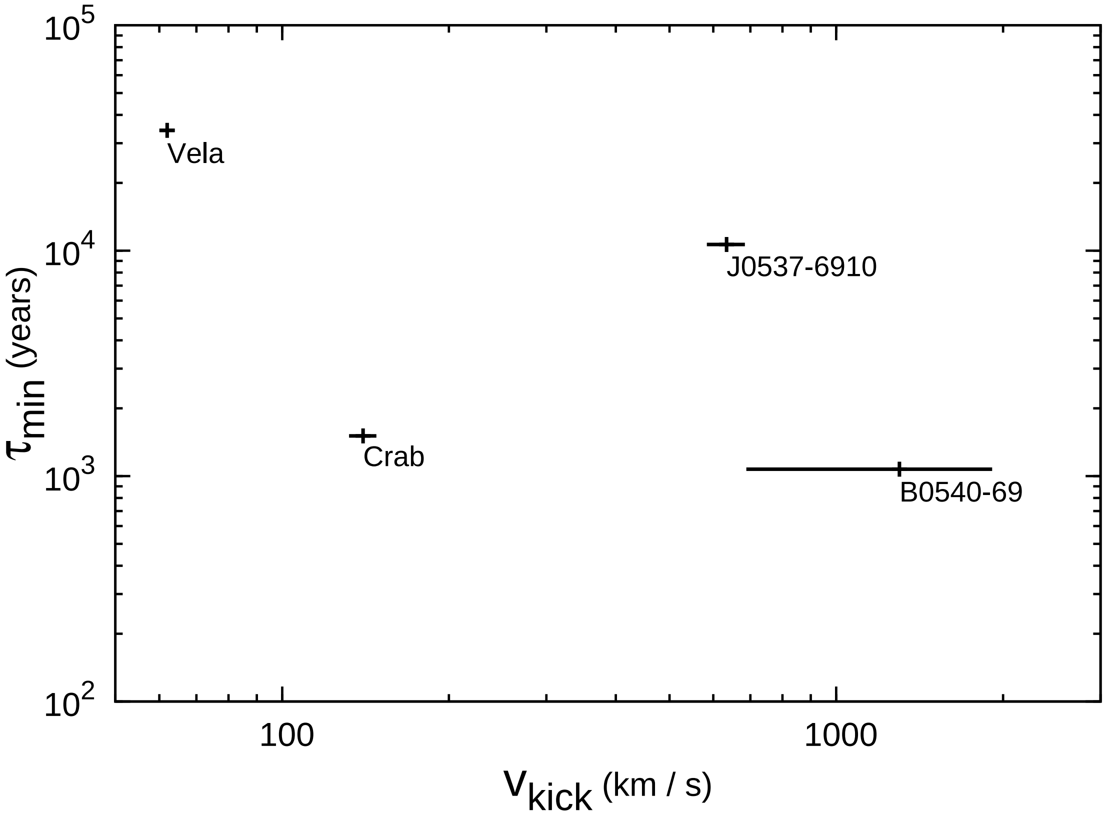

Figure 4.1: The relation between the measured transverse velocities and τmin's of 4 pulsars, B0531+21(Crab), B1509−58, B0833−45(Vela) and B0540−69. These 4 objects form the subset of pulsars with accurately measured braking indices and pulsars with measured transverse velocities. Unfortunately, inverse relation which is expected if the growth of the dipole field is due to the diffusion of the fallback induced submergence of the magnetic field to the surface of the neutron star as neutron stars with large velocities will accrete less and have their fields shallowly submerged, can not be obtained.

5. DISCUSSION

In this thesis we studied the implications of the diffusion to the surface of buried magnetic fields on the spin parameters of rotationally powered pulsars. We predicted that there should be an inverse relation between the growth timescale and the transverse velocities of pulsars assuming the model is correct. We determined the field growth parameters, τ, $\mu_{\rm min}$ and $\mu_{\rm max}$ of the Crab pulsar by exploiting the precisely known true age of this object and its measured second deceleration parameter. We have found that the magnetic moment of the Crab pulsar has to change only a factor of 1.31 indicating that the field of this object has been submerged only shallow probably because it has accreted a small amount of fallback material.

For B0833−45 (Vela), B0540−69, J0537−6910 and J1846−0258 which lack m measurement but have measured braking indices and estimations for their true ages, we determined the minimum value of allowed $\mu_{\rm max}/\mu_{\rm min}$ ratios, which are 4.90, 1.40, 10.5 and 1.83, respectively. Following the method explained in Section 3.2, one finds $(\mu_{\rm max}/\mu_{\rm min})_{\rm min} = 1.28$ for the Crab Pulsar; which is smaller than the values determined for the 4 pulsars lacking m measurement. Especially $(\mu_{\rm max}/\mu_{\rm min})_{\rm min} = 10.5$ for J0537−6910, can provide motivation for future works questioning even transition from CCOs to magnetars.

REFERENCES

[1] **Manchester, R.N.**, **Hobbs, G.B.**, **Teoh, A. and Hobbs, M.**, 2005. The Australia Telescope National Facility Pulsar Catalogue, *The Astronomical Journal*, **129**, 1993–2006, `arXiv:astro-ph/0412641`.

[2] **Baade, W. and Zwicky, F.**, 1934. Cosmic Rays from Super-novae, *Proceedings of the National Academy of Science*, **20**, 259–263.

[3] **Staelin, D.H. and Reifenstein, III, E.C.**, 1968. Pulsating Radio Sources near the Crab Nebula, *Science*, **162**, 1481–1483.

[4] **Hewish, A.**, **Bell, S.J.**, **Pilkington, J.D.H.**, **Scott, P.F. and Collins, R.A.**, 1968. Observation of a Rapidly Pulsating Radio Source, *Nature*, **217**, 709–713.

[5] **Gold, T.**, 1968. Rotating Neutron Stars as the Origin of the Pulsating Radio Sources, *Nature*, **218**, 731–732.

[6] **Lyne, A.G.**, **Pritchard, R.S. and Graham-Smith, F.**, 1993. Twenty-Three Years of Crab Pulsar Rotational History, *Monthly Notices of the Royal Astronomical Society*, **265**, 1003.

[7] **Livingstone, M.A.**, **Kaspi, V.M.**, **Gavriil, F.P.**, **Manchester, R.N.**, **Gotthelf, E.V.G. and Kuiper, L.**, 2007. New phase-coherent measurements of pulsar braking indices, *Applied Surface Science*, **308**, 317–323, `arXiv:astro-ph/0702196`.

[8] **Weltevrede, P.**, **Johnston, S. and Espinoza, C.M.**, 2011. The glitch-induced identity changes of PSR J1119-6127, *Monthly Notices of the Royal Astronomical Society*, **411**, 1917–1934, `1010.0857`.

[9] **Espinoza, C.M.**, **Lyne, A.G.**, **Kramer, M.**, **Manchester, R.N. and Kaspi, V.M.**, 2011. The Braking Index of PSR J1734-3333 and the Magnetar Population, *The Astrophysical Journal Letters*, **741**, L13, `1109.2740`.

[10] **Middleditch, J.**, **Marshall, F.E.**, **Wang, Q.D.**, **Gotthelf, E.V. and Zhang, W.**, 2006. Predicting the Starquakes in PSR J0537-6910, *Astrophysical Journal*, **652**, 1531–1546, `arXiv:astro-ph/0605007`.

[11] **Lyne, A.G.**, **Pritchard, R.S.**, **Graham-Smith, F. and Camilo, F.**, 1996. Very low braking index for the Vela pulsar, *Nature*, **381**, 497–498.

[12] **Ng, C.Y. and Romani, R.W.**, 2006. Proper Motion of the Crab Pulsar Revisited, *Astrophysical Journal*, **644**, 445–450, `arXiv:astro-ph/0602255`.

[13] **Livingstone, M.A. and Kaspi, V.M.**, 2011. Long-term X-Ray Monitoring of the Young Pulsar PSR B1509-58, *Astrophysical Journal*, **742**, 31, 1110.1312.

[14] **Ng, C.Y. and Romani, R.W.**, 2007. Birth Kick Distributions and the Spin-Kick Correlation of Young Pulsars, *Astrophysical Journal*, **660**, 1357–1374, arXiv:astro-ph/0702180.

[15] **Dodson, R.**, **Legge, D.**, **Reynolds, J.E. and McCulloch, P.M.**, 2003. The Vela Pulsar's Proper Motion and Parallax Derived from VLBI Observations, *Astrophysical Journal*, **596**, 1137–1141, arXiv:astro-ph/0302374.

[16] **Gradari, S.**, **Barbieri, M.**, **Barbieri, C.**, **Naletto, G.**, **Verroi, E.**, **Occhipinti, T.**, **Zoccarato, P.**, **Germanã, C.**, **Zampieri, L. and Possenti, A.**, 2011. The optical light curve of the Large Magellanic Cloud pulsar B0540-69 in 2009, *Monthly Notices of the Royal Astronomical Society*, **412**, 2689–2694, 1012.0738.

[17] **Wang, Q.D. and Gotthelf, E.V.**, 1998. ROSAT and ASCA Observations of the Crab-like Supernova Remnant N157B in the Large Magellanic Cloud, *Astrophysical Journal*, **494**, 623, arXiv:astro-ph/9708087.

[18] **Marsden, D.**, **Lingenfelter, R.E. and Rothschild, R.E.**, 2002. Resolution of the age discrepancies in pulsar/SNR associations., *Memorie della Societa Astronomica Italiana*, **73**, 566–571, arXiv:astro-ph/0102049.

[19] **Blandford, R.D. and Romani, R.W.**, 1988. On the interpretation of pulsar braking indices, *Monthly Notices of the Royal Astronomical Society*, **234**, 57P–60P.

[20] **Manchester, R.N. and Peterson, B.A.**, 1989. A braking index for PSR 0540-69, *The Astrophysical Journal Letters*, **342**, L23–L25.

[21] **Alpar, M.A.**, **Ankay, A. and Yazgan, E.**, 2001. Pulsar Spin-down by a Fallback Disk and the P-P Diagram, *The Astrophysical Journal Letters*, **557**, L61–L65, arXiv:astro-ph/0104287.

[22] **Menou, K.**, **Perna, R. and Hernquist, L.**, 2001. Disk-assisted Spin-down of Young Radio Pulsars, *The Astrophysical Journal Letters*, **554**, L63–L66, arXiv:astro-ph/0103326.

[23] **Michel, F.C. and Dessler, A.J.**, 1981. Pulsar disk systems, *Astrophysical Journal*, **251**, 654–664.

[24] **Morley, P.D.**, 1993. Pulsar Braking Index and Mass Accretion, *ArXiv Astrophysics e-prints*, arXiv:astro-ph/9311036.

[25] **Chen, W.C. and Li, X.D.**, 2006. Why the braking indices of young pulsars are less than 3?, *Astronomy & Astrophysics*, **450**, L1–L4, arXiv:astro-ph/0603012.

[26] **Bernal, C.G. and Page, D.**, 2011. Growing Magnetic Fields in Central Compact Objects, Revista Mexicana de Astronomia y Astrofisica Conference Series, volume 40 of *Revista Mexicana de Astronomia y Astrofisica Conference Series*, pp.149–150.

[27] **Melatos, A.**, 1997. Spin-down of an oblique rotator with a current-starved outer magnetosphere, *Monthly Notices of the Royal Astronomical Society*, **288**, 1049–1059.

[28] **Wu, F.**, **Xu, R.X. and Gil, J.**, 2003. The braking indices in pulsar emission models, *Astronomy & Astrophysics*, **409**, 641–645, `arXiv:astro-ph/0307359`.

[29] **Colgate, S.A.**, 1971. Neutron-Star Formation, Thermonuclear Supernovae, and Heavy-Element Reimplosion, *Astrophysical Journal*, **163**, 221.

[30] **Geppert, U.**, **Page, D. and Zannias, T.**, 1999. Submergence and re-diffusion of the neutron star magnetic field after the supernova, *Astronomy & Astrophysics*, **345**, 847–854.

[31] **Michel, F.C.**, 1994. A Fast Pulsar in Supernova 1987A, *Monthly Notices of the Royal Astronomical Society*, **267**, L4.

[32] **Muslimov, A. and Page, D.**, 1995. Delayed switch-on of pulsars, *The Astrophysical Journal Letters*, **440**, L77–L80.

[33] **Chevalier, R.A.**, 1989. Neutron star accretion in a supernova, *Astrophysical Journal*, **346**, 847–859.

[34] **Colpi, M.**, **Shapiro, S.L. and Wasserman, I.**, 1996. Spherical Accretion in a Uniformly Expanding Universe, *Astrophysical Journal*, **470**, 1075.

[35] **Muslimov, A. and Page, D.**, 1996. Magnetic and Spin History of Very Young Pulsars, *Astrophysical Journal*, **458**, 347, `arXiv:astro-ph/9505116`.

[36] **Ho, W.C.G.**, 2011. Evolution of a buried magnetic field in the central compact object neutron stars, *Monthly Notices of the Royal Astronomical Society*, **414**, 2567–2575, `1102.4870`.

[37] **Mereghetti, S.**, 2008. The strongest cosmic magnets: soft gamma-ray repeaters and anomalous X-ray pulsars, *Astronomy & Astrophysics Review*, **15**, 225–287, `0804.0250`.

[38] **de Luca, A.**, 2008. Central Compact Objects in Supernova Remnants, **C. Bassa, Z. Wang, A. Cumming, & V. M. Kaspi**, editor, 40 Years of Pulsars: Millisecond Pulsars, Magnetars and More, volume983 of *American Institute of Physics Conference Series*, pp.311–319, `0712.2209`.

[39] **Halpern, J.P. and Gotthelf, E.V.**, 2010. Spin-Down Measurement of PSR J1852+0040 in Kesteven 79: Central Compact Objects as Anti-Magnetars, *Astrophysical Journal*, **709**, 436–446, `0911.0093`.

[40] **Shabaltas, N. and Lai, D.**, 2011. The Hidden Magnetic Field of The Young Neutron Star in Kesteven 79, *ArXiv e-prints*, `1110.3129`.

[41] **Urpin, V.A. and Muslimov, A.G.**, 1992. Crustal magnetic field decay and neutron star cooling, *Monthly Notices of the Royal Astronomical Society*, **256**, 261–268.

[42] **Cuofano, C.**, **Drago, A. and Pagliara, G.**, 2012. Growth of magnetic fields in accreting millisecond pulsars: the case of J1823-3021A, *ArXiv e-prints*, `1203.1008`.

APPENDICES

APPENDIX A : Plots for the Pulsars Lacking One Measurement

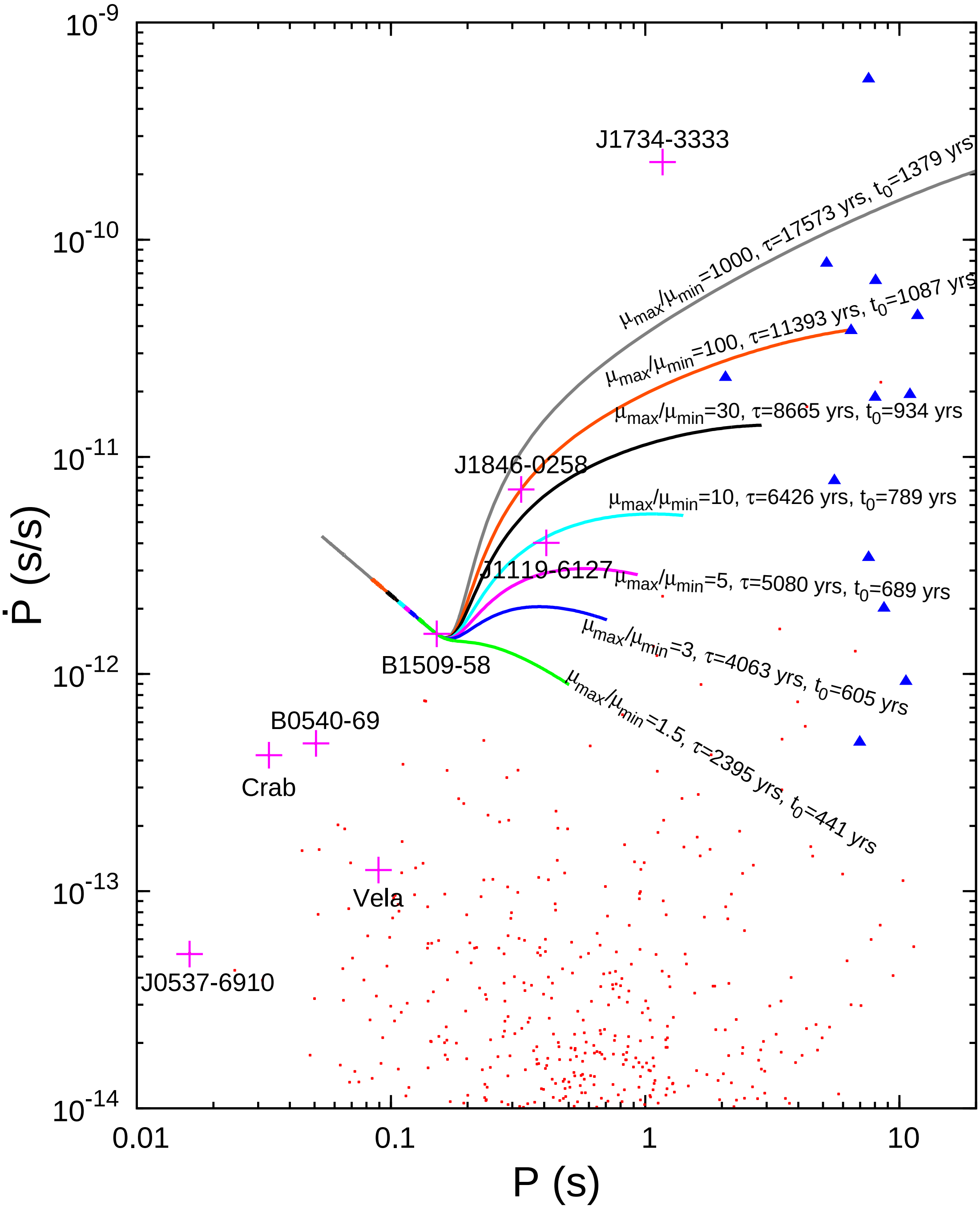

Figure A.1: Evolution of B1509-58 on $P-\dot{P}$ diagram for different $\mu_{\rm max}/\mu_{\rm min}$ ratios from $t=1$ year to $t=10^4$ years. t_0 is also written on each line showing age estimations correspond drawn $\mu_{\rm max}/\mu_{\rm min}$ ratios.

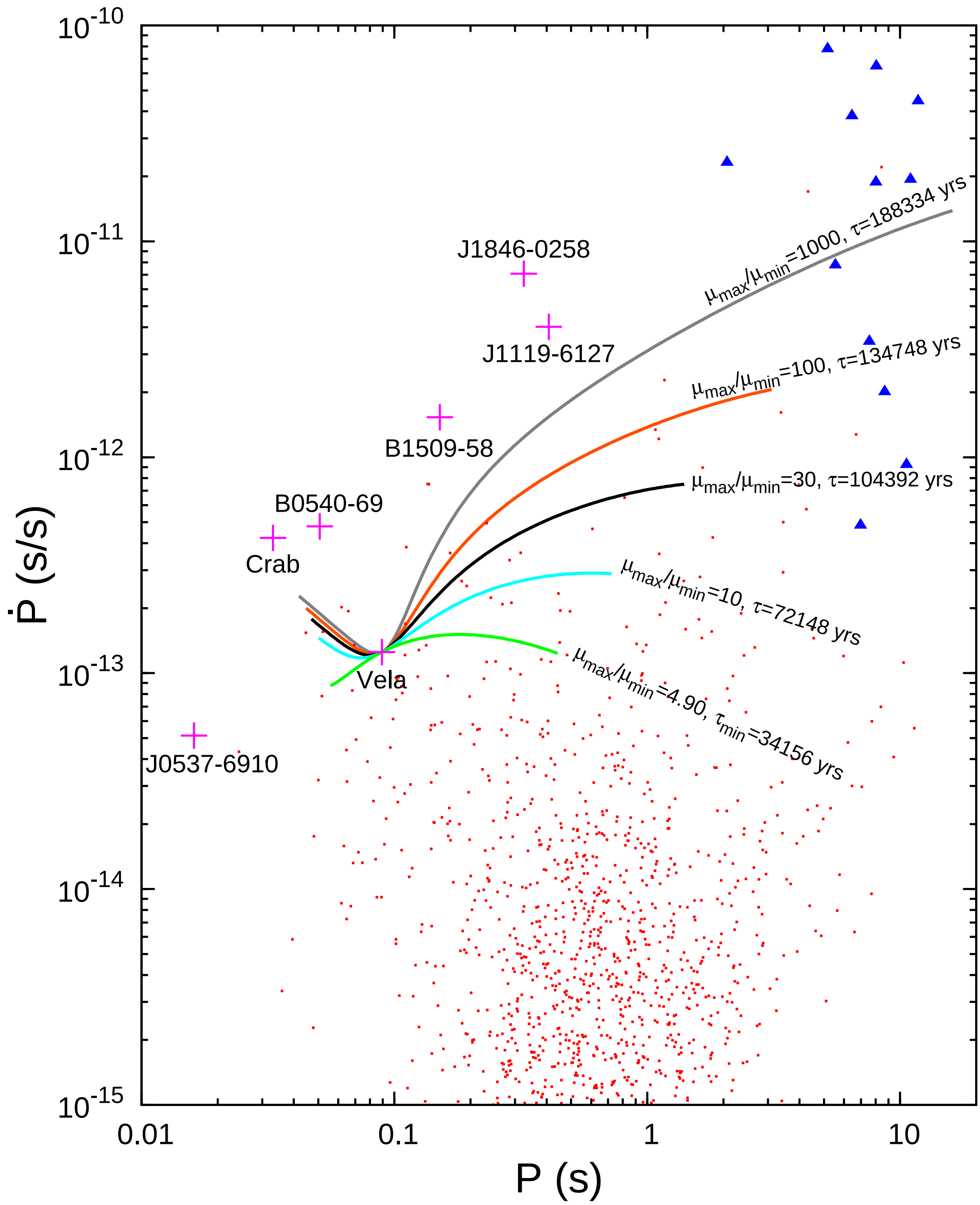

Figure A.2: Evolution of Vela Pulsar (B0833-45) on $P-\dot{P}$ diagram for different $\mu_{\rm max}/\mu_{\rm min}$ ratios from $t=10^4$ years to $t=10^5$ years.

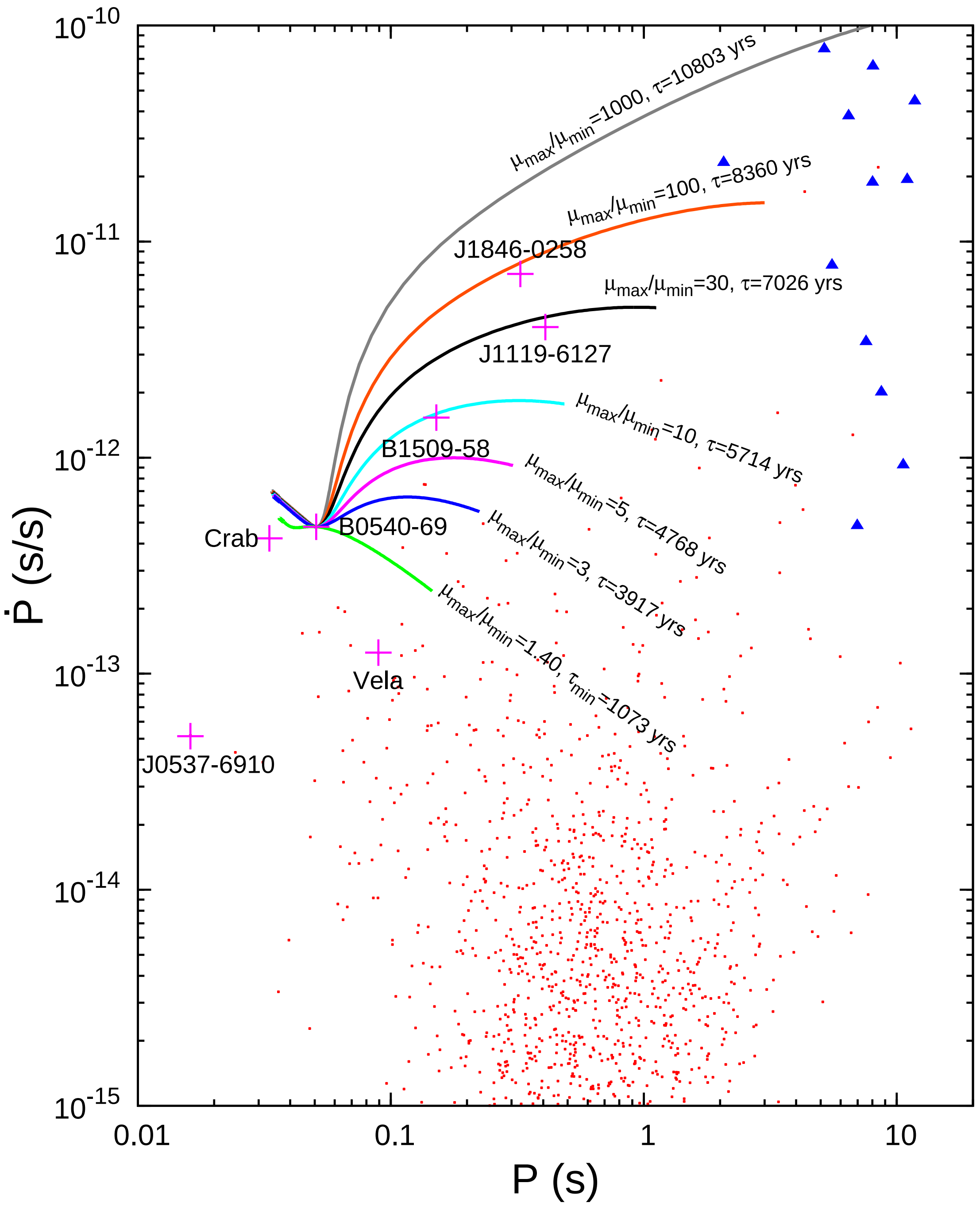

Figure A.3: Evolution of B540-69 on $P-\dot{P}$ diagram for different $\mu_{\max}/\mu_{\min}$ ratios from $t=1$ year to $t=10^4$ years.

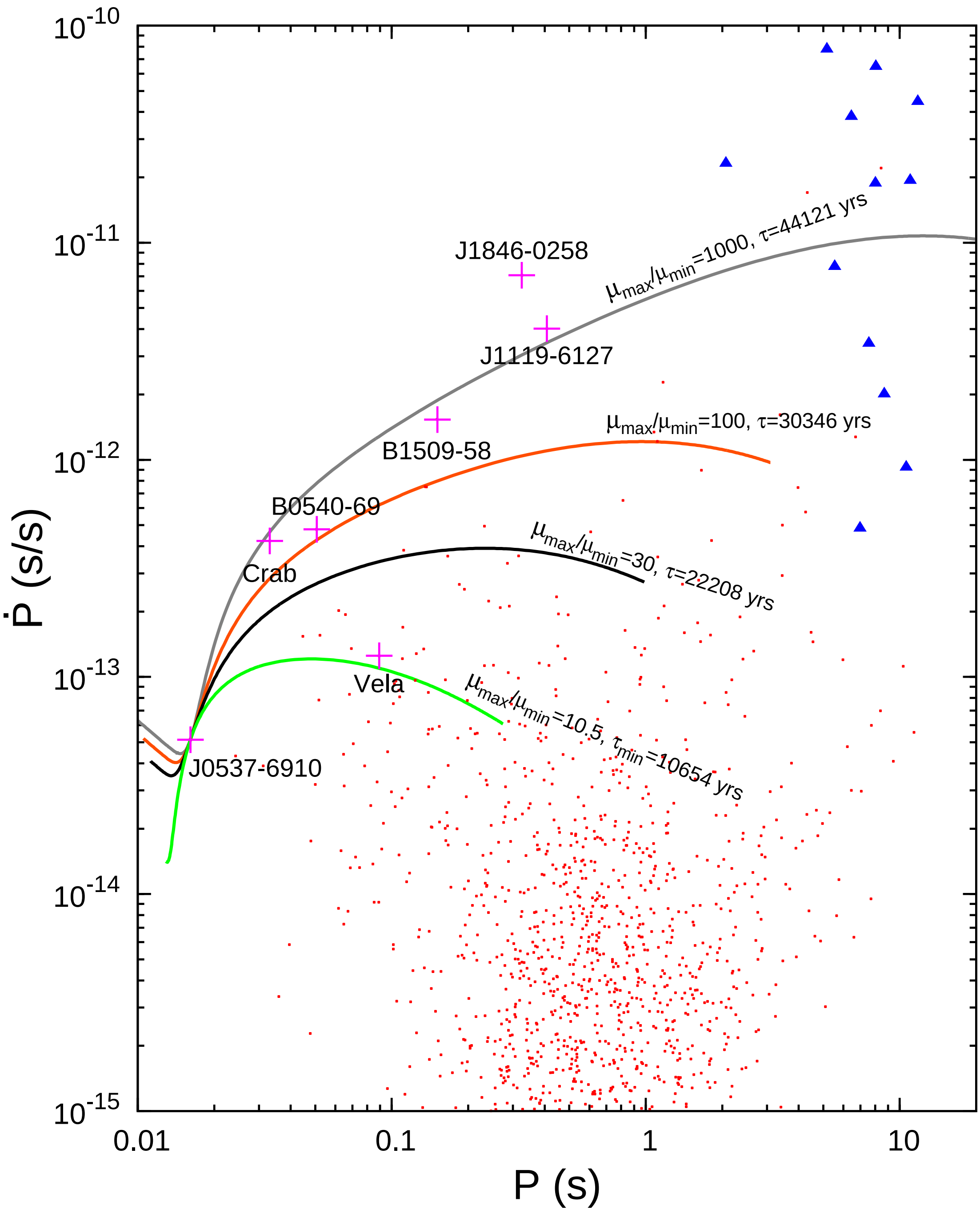

Figure A.4: Evolution of J0537-6910 on $P-\dot{P}$ diagram for different $\mu_{\max}/\mu_{\min}$ ratios from $t = 10^3$ years to $t = 10^5$ years.

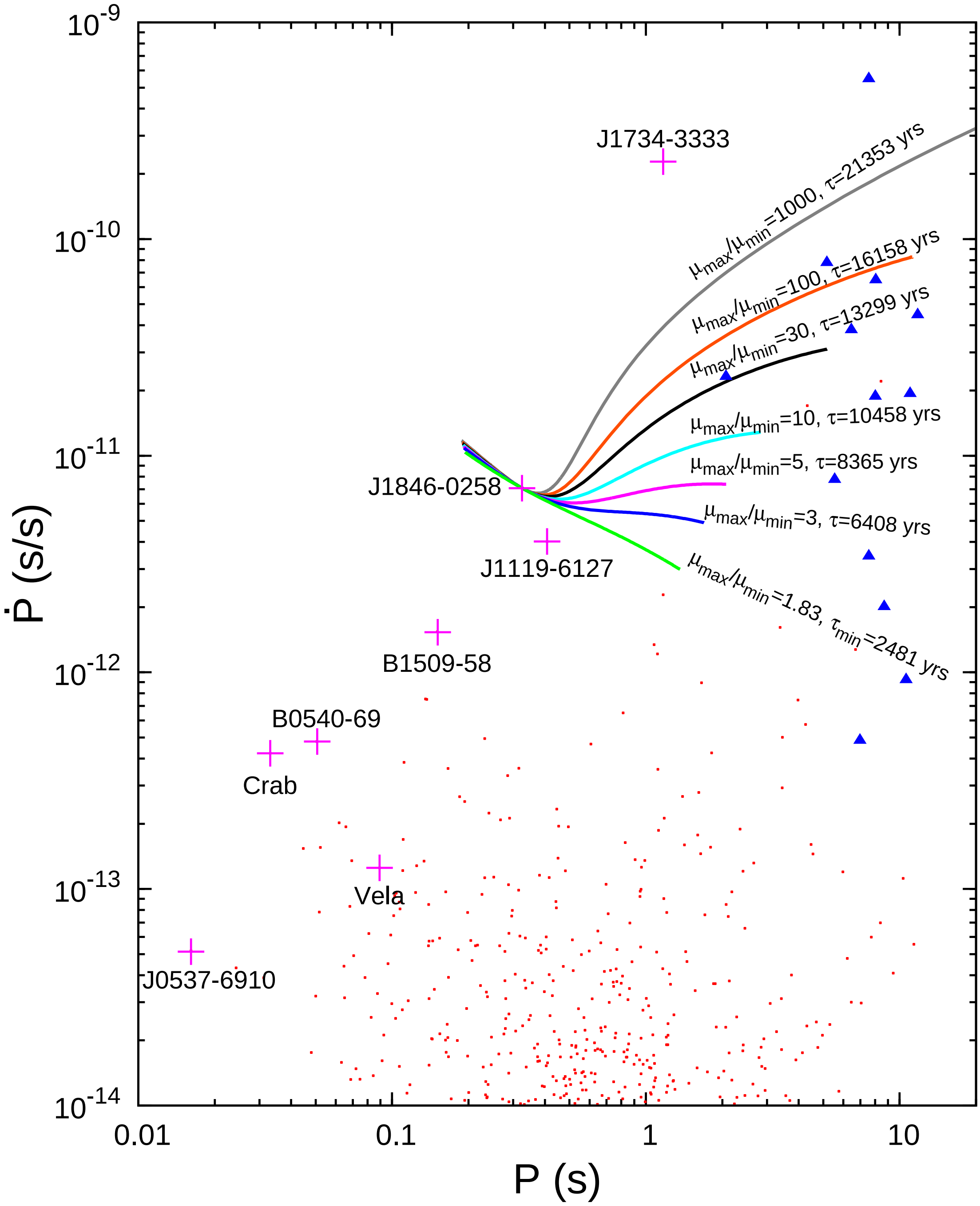

Figure A.5: Evolution of J1846-0258 on $P-\dot{P}$ diagram for different $\mu_{\max}/\mu_{\min}$ ratios from $t = 1500$ years to $t = 10^4$ years.

CURRICULUM VITAE

Name Surname: Abdullah Güneydaş

Place and Date of Birth: İstanbul, 19.09.1985

E-Mail: guneydas@gmail.com

B.Sc.: Bilkent University, Physics Department, May 2009